



HAL
open science

Experimental Flash Pyrolysis of High Density PolyEthylene under Hybrid Propulsion Conditions

Nicolas Gascoin, Guillaume Fau, Philippe Gillard, Alexandre Mangeot

► **To cite this version:**

Nicolas Gascoin, Guillaume Fau, Philippe Gillard, Alexandre Mangeot. Experimental Flash Pyrolysis of High Density PolyEthylene under Hybrid Propulsion Conditions. *Journal of Analytical and Applied Pyrolysis*, 2013, pp.1-11. 10.1016/j.jaap.2013.02.014 . hal-00796085

HAL Id: hal-00796085

<https://hal.science/hal-00796085>

Submitted on 1 Mar 2013

HAL is a multi-disciplinary open access archive for the deposit and dissemination of scientific research documents, whether they are published or not. The documents may come from teaching and research institutions in France or abroad, or from public or private research centers.

L'archive ouverte pluridisciplinaire **HAL**, est destinée au dépôt et à la diffusion de documents scientifiques de niveau recherche, publiés ou non, émanant des établissements d'enseignement et de recherche français ou étrangers, des laboratoires publics ou privés.

1 Experimental Flash Pyrolysis of High Density 2 PolyEthylene under Hybrid Propulsion Conditions

3 Nicolas Gascoin^{1*}, Guillaume Fau¹, Philippe Gillard¹, Alexandre Mangeot^{1,2}

4 ¹*University of Orléans, 63 avenue de Lattre de Tassigny, 18020 Bourges, France*

5 ²*Centre National d'Etudes Spatiales, Rond Point de l'Espace, 91023 Evry Cedex, France*

6 **The inert and oxidative flash pyrolysis of High Density Poly-Ethylene (HDPE) is studied**
7 **up to 20 000 K.s⁻¹, under pressure up to 3.0 MPa and at temperature ranging from 1000 K to**
8 **1500 K. These conditions are considered to represent those waited onboard a hybrid rocket**
9 **engine using HDPE as solid fuel. Recycling applications may also find some interest. The**
10 **pyrolysis products are quantified by Gas Chromatograph, Flame Ionisation Detector and**
11 **Mass Spectrometer to determine the effects of each physical parameter on the HDPE**
12 **decomposition. The classical products distribution diene-alkene-alkane for each carbon**
13 **atoms number is shown to be modified at such high temperature because of the pyrolysis of**
14 **primary products. The pressure effect, which is generally neglected in HDPE pyrolysis**
15 **studies found in open literature, is proved to be a major factor (up to one order of**
16 **magnitude on the ethylene mass fraction). The heating rate presents noticeable consequences**
17 **on the pyrolysis products distribution with a larger formation of light species while heavier**
18 **ones are favoured under oxidative pyrolysis conditions. The experimental data should serve**
19 **in the future to improve the accuracy of kinetic mechanisms for later use in numerical**
20 **computing and to serve in related combustion studies for propulsive applications.**

* Corresponding author : nicolas.gascoin@univ-orleans.fr, Tenure Professor, Tel.: +33 248 238 473; Fax: +33 248 238 471, 63 avenue de Lattre de Tassigny, 18020 Bourges Cedex FRANCE

21 **Keywords: Polyethylene; flash pyrolysis; heating rate and pressure effects; design of experiments; hybrid**
22 **propulsion.**

23 **1. Introduction**

24 High Density Polyéthylène (HDPE) is presently of high interest in numerous civil applications of daily life,
25 which explains the number of works related to its recycling [1]-[5]. In addition, this polymeric material may be of
26 interest for hybrid rocket propulsion [6] despite this solid fuel presents one major drawback. Indeed, its low
27 regression rate makes the combustible generation to be too low to provide interesting thrust [7]. Summarising the
28 fundamentals of hybrid engine, it can be recap that the solid fuel constitutes the combustion chamber in which the
29 oxidiser is injected. For this reason, the combustion generates the heat flux which serves to pyrolyse the fuel and to
30 produce the gaseous combustible fuel [7]. A complex phenomenology occurs at the solid surface with regression,
31 diffusion flame and possible melting layer with spray generation when using liquefying fuel [7].

32 It is hoped to cope the weak point of the low HDPE regression rate by the transient production of light
33 compounds with low auto-ignition delay. Indeed, it was found in previous work that the nature of the chemical
34 species produced by the fuel pyrolysis changes depending on the pyrolysis conditions [8]. Hence, it may be possible
35 to produce chemical compounds with low auto-ignition delay which would burn close to the solid regression
36 surface[9]. This would reinforce the heat transfer and thus the fuel pyrolysis. As a consequence, this would increase
37 the regression rate. **Thus, it is required to conduct an adequate experimental study to determine in which**
38 **conditions, such species would be favoured.**

39 Firstly, low heating rates are generally encountered in open experimental literature since Thermogravimetric
40 analysis or other conventional experimental devices are used to ensure the thermal degradation [4],[10],[11]. For this
41 reason, **a flash pyrolysis system should be preferred.** Secondly, the operating pressures are often far from those
42 encountered in real hybrid rocket engine conditions (over 3 MPa) but merely the atmospheric one [12]. Last, the
43 maximum temperature found in existing pyrolysis works is reported by Elordi *et al.* (988 K) [13] while the one
44 expected in hybrid combustor easily overpasses 1000 K [14]. Some works considering combustion of HDPE also
45 consider higher temperature but the two chemical regimes (pyrolysis/combustion) are not easily isolated [7], [9],
46 [15]. Consequently, a clear lack of data is found for the specific conditions to be found in hybrid engines. This

47 justifies the present work which should provide data for a later use in numerical computations and kinetic
48 mechanisms conception.

49 Numerically, a limited number of detailed kinetic schemes is found for HDPE [12], [16]. Mastral *et al.* reported
50 the lack of appropriate pyrolysis data for HDPE [10]. Most of the chemical mechanisms lump the gas species into a
51 single one and similarly for the solid and liquid phases [2], [3], [17]-[19]. Some work even consider a single
52 degradation step for the polyethylene [20], [21]. This may be of interest for recycling purpose to find the optimum
53 valuing conditions but this is not appropriate for aerospace applications. A gas species can be methane or acetylene,
54 which is absolutely different from a combustion point of view (several orders of magnitude on the auto-ignition
55 delay) [22]. Thus, the identification of each compound requires a detailed kinetic mechanism. A reduction work has
56 conducted to such a scheme with 1713 reactions and 472 species instead of 7541 reactions and 1014 species [23].
57 This kinetic scheme is intended to be used in Computational Fluid Dynamics code [14] but it requires being
58 validated first under operating conditions in agreement with those expected on the hybrid rocket engine. In this
59 perspective, the experimental data to be obtained in the present work should be determining.

60 Finally, from a fundamental point of view, additional data related to the HDPE pyrolysis could be fruitful to
61 analyse the main chemical pathway of reactions. The main ones are well-known and have been described by
62 Wampler [24]. Initiation reactions generate by random scission the primary radicals which then form alkenes by β -
63 scission and alkanes by H-abstraction when reacting with the polymeric molecule. Similar reactions conduct to
64 diene formation. The typical products distribution profile shows triple peaks for each carbon atom number. Each of
65 the primary products is then pyrolysed depending on the test conditions. The relative concentration of each chemical
66 group then varies while it is initially linearly linked with the carbon atom number [25]. Further details on HDPE
67 pyrolysis and associated kinetic schemes can be found in Ref. [23].

68 **This work aims at furnishing reliable pyrolysis data for HDPE under unexplored conditions, which are**
69 **those encountered onboard a hybrid engine. For this purpose, it relies on flash-pyrolysis experiments;**
70 **coupled to additional ThermoGravimetry analysis to estimate the pyrolysis rate as a function of the**
71 **temperature. The effects of the physical parameters on the HDPE pyrolysis and on the products formation**
72 **are investigated through a design of the experiment. A deep quantification work is carried out on the product**
73 **formation.**

74 **2. Materials and methods**

75 The HDPE is sourced from Politek (PE1000). On the basis of the data furnished by the manufacturer, the HDPE
76 presents the following main characteristics: white colour, density of 940 kg.m^{-3} and thermal conductivity of
77 $0.38 \text{ W.m}^{-1}.\text{K}^{-1}$. In addition, a large characterisation work has been achieved prior to the present study in order to
78 have all the properties which would be suitable for engineering and scientific uses of this HDPE. These data are
79 given in section 3.1.

80 **2.1. Pyrolysis devices**

81 A high pressure flash pyrolysis system (CDS, 5200 HP) has been connected to a Gas Chromatograph (Varian,
82 3800 with Varian MS Workstation 6.9 software) equipped with a Flame Ionisation Detector in parallel to a Mass
83 Spectrometer (Varian, Saturn 4000 with ion trap). A Platinum coil is electrically heated to heat the sample placed
84 within a quartz tube. The flash pyrolyser is used in trap-mode, which enables accumulating the pyrolysis products on
85 a triple-bed trap (CDS, 90mg-60:80-Tenax-TATM/Carboxen 1000/CarbosieveTM SIII) before flushing the species to
86 the GC through the split/splitless injector (Varian, 1177, internal volume: 0.95 ml). Helium is used as carrier gas
87 with a constant flow rate of 30 ml.min^{-1} (independent from the operating conditions). This corresponds to a
88 residence time for volatiles around 1 s in the system. Fused silica (Agilent, 0.32 mm, 10 m) with a split ratio 1/10 is
89 used to equilibrate the flows between the two detectors. A GS-CARBONPLOT column (Agilent, 0.32 mm, 30 m,
90 3.0) is connected on the FID to separate the light compounds (C1-C8). A VF-5ht column (Agilent, 0.32 mm, 30 m,
91 0.10) is placed on the MS line to separate the heavy species (C8-C26). A quantification work (detailed in next
92 section) allows determining the quantity of each pyrolysis product.

93 Apart the above process-analysis coupled device, a ThermoGravimetry apparatus has been employed
94 (SETARAM, Setsys 16/18). It enables weighting solid samples during thermal degradation up to 2000 K. Argon has
95 been used as carrier gas and alumina crucible served to deposit the HDPE sample. Initial and final weights of
96 samples were controlled by a mass balance to confirm the TG data. The pyrolysis rate (consumed mass of sample
97 divided by the initial one) is expressed so as to the regression rate (consumed mass of HDPE over the time of
98 consumption). The regression rate is converted in mm.s^{-1} instead of mg.s^{-1} as measured by the TG by assuming
99 cubic samples.

100 **2.2. Test conditions and Design of experiments**

101 A two-level design of experiments [26] is proposed to determine the effects and their quantitative importance on
102 the HDPE pyrolysis with the flash pyrolysis device (Table 1). An additional temperature has been added (1250 K)
103 between the two levels (1000 K and 1500 K) to provide temperature dependence profile of the species
104 formation/consumption. The programming of the flash pyrolysis consists in a heating with a slope equal to the
105 heating rate to reach the final temperature. After 15 s of thermal plateau at this maximum temperature (during which
106 the pyrolysis species are trapped thanks to the flow of reactant gas), the trap is desorbed during 2 min with He. The
107 transfer line to the GC is heated to 623 K (same desorption temperature as the trap).

108 *Table 1 should be placed here*

109 A calibration of the GC detectors has been achieved prior to the experiments to identify and quantify the
110 products. For this purpose, standards have been injected with different successive dilution factors. To limit the
111 quantification work, 44 species ranging from C1 to C26 are analysed (including the main possible chemical groups:
112 diene, alkene, alkane). These species are the major one observed during the experiments. Tens to hundreds other
113 species are found under negligible quantities (< 50 ppm). The MS parameters are the classical ones [28] with a scan
114 from 15 to 350 m/z ratio. The GC thermal programming is isothermal at 303 K during 3 min before a slope at
115 20 K.min⁻¹ up to 623 K and then a thermal plateau during about 30 min.

116 Finally, the TG programming includes a thermal plateau at 303 K during 30 min, then a heating with a slope of
117 20 K.min⁻¹ and finally a last thermal plateau of 30 min at the maximum desired setup temperature (633 K to 773 K
118 by step of 20 K). Two reactant gases (inert with Argon or oxidative with Air) are used to qualify the atmosphere
119 effect.

120 **3. Results and Discussion**

121 **3.1. Characterisation of the HDPE sample and tests repeatability**

122 A preliminary characterisation of the HDPE has been done despite it is not the aim of the present work. A
123 coupled analysis has been achieved by Fourier Transform Infrared spectrometer (Diffuse reflection) and Electron
124 Dispersive Scanning (with Scanning Electronic Microscope). Negligible presence of phenol additives is suspected.
125 Differential Scanning Calorimeter (DSC) analysis confirmed a melting point around 138 °C, a fusion enthalpy of
126 205 J.g⁻¹ ± 31 J.g⁻¹ and the crystallinity of the polymer was estimated to reach 72 % ± 11 %. To get this last value, the

127 method consisting in dividing the fusion enthalpy by the HDPE theoretical one (285 J.g^{-1}) was used. The main
128 results are given in Ref. [27].

129 Concerning the experiments, the test repeatability has been verified by three to four successive experiments in
130 the same conditions with both apparatus (TG and flash pyrolyser). Regarding the TG results (Figure 1a), the final
131 conversion rate is reproducible but the larger the sample, the slower the conversion. Here, mass from 0.85 mg to
132 almost 6 mg have been tested. This observation is well-known and it is linked to the thermal heterogeneity when the
133 sample is too large. Concerning the flash pyrolysis system (Figure 1b), a large repeatability study has been achieved
134 systematically concerning the apparatus and concerning the size of the samples. Because of the numerous species
135 and the difficulty to properly separate each peaks of the chromatogram and of the mass spectrogram, a disagreement
136 up to 20 % can be found for some species while it is generally less than 5 %. For this reason, it has been preferred to
137 determine the average value after three tests for each condition. This method is the one used in the present study and
138 the results given later will be those of the mean value. The reason of the discrepancies has been investigated. It is
139 first due to the ability of the authors to produce constant samples mass and shape. Regarding the size of the solid
140 sample, it should be limited to few hundreds of microns, which is difficult experimentally. Thus, a large error could
141 be observed without rigorous sample preparation method. Consequently, the samples were prepared by cutting them
142 directly and manually from an initial homogeneous solid block of HDPE. Several tens of samples were prepared and
143 then observed by microscope to quantify their size. Those with a similar size around $400 \mu\text{m}$ were selected. The
144 final dispersion is $\pm 20 \mu\text{m}$. The second main reason of the discrepancies is due to the fact that the pyrolysis products
145 are trapped after being generated by the pyrolysis. Hydrogen is lost through this step. The products are then released
146 by thermo-desorption to the GC/MS analytical device (at 350°C). The heavier species thus may remain in the trap.
147 This impacts the mass balance which cannot be verified during the experiments.

148 *Figure 1 should be placed here*

149 In addition, an extended numerical work has been conducted with analytical laws and multiphysics code (Fluent,
150 Comsol) to determine if the sample temperature within the flash pyrolysis probe dynamically follows the setup
151 temperature, particularly for the high heating rates. It was notably found that even at 20000 K.s^{-1} , the sample
152 temperature reaches the one of the setup after 1 s.

153 **3.2. First pyrolysis data**

154 Inert and oxidative TG experiments from 633 K to 773 K have been achieved (Table 2). The pyrolysis rate
155 reaches 100 % for approximately the same temperature whatever the atmosphere. Nevertheless, the dynamics of the
156 pyrolysis changes between the inert and the oxidative cases. Considering the pyrolysis rate enables estimating the
157 amount of combustible gaseous species which can be produced during the use of hybrid rocket engine depending on
158 the test conditions. The regression rate (either in mm.s^{-1} or in mg.s^{-1}), in addition to the pyrolysis rate, gives
159 additional information on the dynamic of the pyrolysis process. The regression rate in mg.s^{-1} is given directly by TG
160 results while expressing it in mm.s^{-1} is of interest for technologic use in hybrid rocket engine because this allows
161 estimating the combustion port diameter for example. This rate (in mm.s^{-1} for example) is higher for the oxidative
162 pyrolysis and it increases much faster in this condition than in inert condition (Table 2). The ratio between these two
163 tests ranges from 1.6 at 633 K to 6.7 at 773 K (in favour to the oxidative case). The temperature of self ignition for
164 HDPE ranges in the literature from 603 K to 683 K [29]. Thus, it could be assumed that a slow combustion, or
165 oxidation process, occurs during the pyrolysis which enhances the heat transfer and promotes the HDPE
166 consumption. Consequently, this confirms the need to consider the atmosphere in the design of experiments, as
167 proposed in Table 1, to dissociate the thermal effect and the chemical one of the heterogeneous reactions. The
168 oxidation reactions should be clearly seen in DSC through an exothermic peak. It can be noticed that the TG curves
169 under oxidative atmosphere present different slopes with inflexion point around 673 K (3100 s), which tends to
170 confirm the oxidation process and the existence of a HDPE oxidation induction delay (Figure 2).

171 *Table 2 should be placed here*

172 *Figure 2 should be placed here*

173 The regression rate measured with the TG (Figure 4a) clearly differs between inert and oxidative cases as
174 mentioned above. Using a classical Arrhenius law, the pre-exponential factor is found to be equal to $7.52.10^6$ s (for
175 10^8 in Ref. [30]) and the activation energy is 124 kJ.mol^{-1} (for 130 kJ.mol^{-1} in Ref [30]). In addition (Figure 4b), the
176 estimated regression rate in mm.s^{-1} is about 20 times less than the one generally observed in real hybrid rocket
177 conditions [7], that is to say 0.2 mm.s^{-1} . This is attributed to the heating rate and to the temperature of the sample.
178 Indeed, the heating rate in hybrid combustor is estimated around 10^5 K.s^{-1} , much higher than 20 K.min^{-1} in the TG.
179 As a consequence, reaching 1000 K –at least- would demand 35 min with TG device. This time is far too important
180 to be representative of real conditions and this explains why TG tests have been achieved up to 773 K maximum.
181 Furthermore, the fact that the regression rate is higher for the oxidative atmosphere (which takes benefit of
182 additional heat release due to oxidation reaction) demonstrates that a higher heating rate (or heat release rate)

183 promotes the regression rate. For this reason, additional experiments in flash pyrolysis system (up to 2.10^4 K.s^{-1}) are
184 proposed in the following section.

185
186

Figure 3 should be placed here

187 3.3. Parametric study of flash pyrolysis

188 In conformity with the parameters and their respective levels given in the design of experiment (Table 1), the
189 composition of each corresponding pyrolysis mixture is given in Table 3 (each data is the mean value determined
190 after three replicate tests). An example of some mass spectrograms acquired during the analysis of the pyrolysis
191 mixtures is furnished by Figure 5. **The differences between the different test conditions are significant (Table 3)**
192 **since they are higher the reproducibility which has been tested.** The quantities of dienes, alkenes and alkanes are
193 also given to quantify their relative importance at each test condition. Methane and acetylene are found in trace
194 quantity and hydrogen is not quantified for trapping reason. As mentioned in introduction, the classical diene-
195 alkene-alkane triple peak is observed for some carbon atoms number (for example C9 to C13). For some others, for
196 example C8 and C15 and over, it was not possible to isolate the three chemical groups due to co-elution. As a
197 consequence, the three species are lumped into the alkene molecule for quantification purpose. The peak is referred
198 to Cx to clearly mention this point. Since the alkenes are the major compounds, this decreases the error inherited
199 from this correction. It can be noted that the ethylene content decreases when the temperature increases. This is
200 related to its pyrolysis which is favoured at lower pressure.

201 *Table 3 should be placed here*
202 *Figure 4 should be placed here*

203 On the basis of these results, the products formation is plotted versus the temperature to identify the separate
204 effects of the atmosphere (Figure 6), of the pressure (Figure 7) and of the heating rate (Figure 8). Despite only three
205 temperatures were tested, the variations are greater than the uncertainties (marked with error bars) and the discussion
206 of the results justify considering them. The alkene formation is only slightly impacted by the temperature (in the
207 range 60 mol.%-70 mol.%) and even less by the atmosphere (Figure 6). A balance is observed between alkanes and
208 dienes depending on the tested temperature. The alkane formation decrease is compensated by the increase of the
209 diene production. Considering the atmosphere effect, it mostly impacts the dienes and alkanes, with a minimum
210 effect around 1250 K. This point is complex to explain since the chemistry of oxidative pyrolysis implies
211 heterogeneous reactions between the HDPE and the air. The dienes/alkenes/alkanes present molecular weight from

212 low to high value. Some of them are produced and other consumed depending on the temperature and atmosphere.
213 Thus, additional analysis will be provided in next section thanks to the design of experiments.

214 *Figure 5 should be placed here*

215 At higher pressure (3 MPa), the temperature effect is decreased since the dienes, alkenes and alkanes formation
216 fluctuates in a lower extent between 1000 K and 1500 K (Figure 7). The bimolecular reactions do play a role at high
217 pressure -due to the concentration effect of species-. At 3 MPa, the dienes quantity linearly increases with the
218 temperature while the one of alkanes decreases. Similarly, decreasing the heating rate from $2 \cdot 10^4 \text{ K}\cdot\text{s}^{-1}$ to $10^2 \text{ K}\cdot\text{s}^{-1}$
219 results in a linear increase of the dienes quantity (Figure 8). For high temperature level (1500 K), the alkanes
220 formation is lower than at lower temperature, which is balanced by the alkenes one. This fact will be discussed in
221 next section by differentiating light and heavy alkenes whose formation and consumption is not necessarily linked.
222 The application of these results to the hybrid engine technology and their fundamental analysis to improve the use of
223 kinetic chemistry will be detailed.

224 *Figure 6 should be placed here*

225 *Figure 7 should be placed here*

226

227 **3.4. Quantification of parameters effects**

228 The data have been then post-processed according to the design of experiments (example for ethylene in Table
229 4). The parameter levels are those defined in section 2.2 (Table 1). The ethylene content is the one measured
230 experimentally (given in Table 3). The answer to each parameter (last line of each parameter column) is quantified
231 by considering the sum of the eight scalar products (eight test lines in Table 4) between the parameter level (+1 or -
232 1) and the mole fraction of ethylene corresponding to the same test number (last column of Table 4). The main effect
233 appears to be the atmosphere (68.3 % in absolute value), then the heating rate, the pressure and finally the
234 temperature. All these parameters have major impact since they clearly overpass the mean ethylene mole fraction
235 (9.0 % is computed as the mean value of the eight line results in the ethylene column). The fact that the temperature
236 effect is negative demonstrates that at 1500 K, ethylene starts to be pyrolysed (as expressed when comparing tests 1
237 and 7 or 2 and 8 for example). The same qualitative effect is found with the atmosphere (air instead of He) while the
238 opposite is found for the pressure and the heating rate. Similar work has been achieved for the parameters
239 interactions without clear trends, which would tend to demonstrate that these parameters are independent.
240 Nevertheless, an extended work would be necessary to clearly state on this point since the quantification of
241 interactions with a two-level or three-level design of experiments would require additional tests.

242 *Table 4 should be placed here*

243 The results of the design of experiments are summarized for all the species in Table 5. The higher effects are
244 found for ethylene and propylene, then for ethane and propane. The pressure effect is then the highest for the alkenes
245 from C9 to C12 (in absolute value, negative sign), which implicates that related β -scission reactions are penalised at
246 high pressure. To the opposite, the higher heating rate generally favours the alkenes formation (mostly the light
247 ones). The heavier species (C12 and over) are not impacted to the opposite by the heating rate. As a consequence,
248 the overall effect of the heating rate is the one observed in Figure 8. This result is of major importance because this
249 confirms previous results from numerical and experimental multiphysics studies [22], [31]. The light alkenes are
250 formed preferably when the fuel is heated strongly and rapidly; that is to say when the heating rate is high. This
251 point has a direct connection with hybrid rocket since producing light alkenes will result in the decrease of the auto-
252 ignition delay. Thus, the flame front will establish close to the reducer surface and this should enhance the heat
253 transfers, so the regression rate of the fuel.

254 Regarding the atmosphere, it mostly impacts the light species in the sense of consumption when considering air.
255 This is directly due to their combustion due to lower auto-ignition delays compared to other and heavier compounds.
256 Among the 42 species, the pressure effect is the major one for 34 compounds (mainly for those over C7) and the
257 heating rate is the second important parameter for 25 species among these 42 ones. The atmosphere is the major
258 parameter for the lighter species (from C₂H₄ to C₇H₁₄). Surprisingly, the temperature is not the major parameter in
259 the range 1000 K – 1500 K for the studied species but this does not imply that temperature is not an important
260 parameter. Indeed, the temperature presents a higher effect than the mean mole fraction value for 28 species among
261 the 42, which means that it is, in majority, an important parameter. In addition, the pyrolysis appears at much lower
262 temperature than 1000 K (as seen in section 3.1) and this contributed to explain the lower weight of the temperature
263 in these specific conditions.

264 *Table 5 should be placed here*

265
266 **4. Conclusion**

267 Among several applications, hybrid rocket propulsion can take benefice from HDPE pyrolysis studies to estimate
268 the production of species and their nature for later use in combustion. The present study aims at proposing adequate
269 results within this framework. The HDPE pyrolysis rate as been estimated under steady-state TG experiments. The
270 regression rate has been determined as a function of the temperature under inert and oxidative conditions. The

271 oxidation of the products has been shown and it results in a discrepancy of several factors of magnitude between the
272 two atmospheres results. The regression rate appears quite low in TG tests (one to two orders of magnitude
273 compared to real hybrid tests). This is attributed to the low heating rate, temperature and pressure. Thus, using a GC-
274 MS-flash pyrolysis coupling, the conditions of a hybrid engine have been chosen to estimate the parameters effects
275 through a design of experiments from 1000 K to 1500 K, 0.1 MPa to 3 MPa, 10^2 K.s^{-1} to 2.10^4 K.s^{-1} and under inert
276 and oxidative atmosphere. In addition to the clear thermal effect on the pyrolysis products formation, the pressure
277 appears as the second important parameter while the heating rate and the atmosphere also play a noticeable role (in
278 this order of importance). The fact that the heating rate plays a role while the final temperature is reached after one
279 second clearly shows the highly transient behaviour of the pyrolysis. The light alkenes are favoured at high heating
280 rate –contrary to the dienes–, which confirms the previous results. Thanks to a design of experiment, it is found that
281 the pressure impacts negatively the β -scission reactions. The alkanes are pyrolysed preferentially during a
282 temperature increase, particularly for high pressure conditions. These results will now contribute to validate and to
283 improve existing kinetic mechanisms of HDPE pyrolysis since they are unique to the authors' knowledge. Indeed,
284 the data from literature are generally obtained and fitted for conditions up to 1000 K, at ambient atmosphere and low
285 heating rate (less than 1 K.s^{-1}), which need to be improved to match with the requirements of hybrid rocket. A future
286 work could be to use these mechanisms to determine the rate of production of compounds adequate as fuel for the
287 hybrid engine.

288 **Acknowledgements**

289 The authors would like to acknowledge the Roxel company for its financial support.

290 **References**

- 291 [1] S.E. Levine, L.J. Broadbelt, *Polym. Degrad. Stabil.* 94 (2009) 810–822
292 [2] S.M. Al-Salem, P. Lettieri, *Polymer chemical engineering research and design* 88 (2010) 1599–1606
293 [3] R.W.J. Westerhout, J. Waanders, W.P.M. Van Swaaij, *Ind. Eng. Chem. Res.* 37 (6) (1998) 2293–2300
294 [4] M. D. Wallis, Suresh K. Bhatia, *Polym. Degrad. Stabil.*, 92 (2007) 1721-1729
295 [5] A. Aboulkas, K. El harfi, A. El Bouadili, *Thermochim. Acta* 500 (2010) 30–37
296 [6] N. Gascoin, P. Gillard, A. Mangeot, A. Navarro-Rodriguez, *J. Anal. Appl. Pyrolysis*, 94 (2012) 33–40
297 [7] M.J. Chiaverini, K.K. Kuo, *Fundamentals of hybrid rocket combustion and propulsion*, vol. 218, Published by
298 the American Institute of Aeronautics and Astronautics, Reston, Virginia.
299 [8] N. Gascoin, P. Gillard, A. Mangeot, A. Navarro-Rodriguez, *J. Anal. Appl. Pyrolysis*, 94 (2012) 1–9
300 [9] K. Soojong, L. Jungpyo, M. Heejang, S. Honggye, K. Jinkon, C. Jungtae. 46th AIAA/ASME/SAE/ASEE Joint
301 Propulsion Conference & Exhibit, 2010, AIAA-2010-7031.
302 [10] J.F. Mastral, C. Berruero, J. Ceamanos, *J. Anal. Appl. Pyrolysis* 79 (2007) 313–322
303 [11] C. Dong, Y. Yang, B. Jin, M. Horio, *Waste Manage.*, 27(11) (2007) 1557–1561
304 [12] A. Németh, M. Blazso, P. Baranyai, T. Vidoczy, *J. Anal. Appl. Pyrolysis* 81 (2008) 237–242
305 [13] G. Elordi, G. Lopez, M. Olazar, R. Aguado, J. Bilbao, *J. Hazard. Mater.* 144 (2007) 708–714

- 306 [14] A. Mangeot, N. Gascoin, P. Gillard, 20th AIAA Computational Fluid Dynamics Conference, 2011, AIAA-
307 2011-3212
- 308 [15] P. Grammelis, P. Basinas, A. Malliopoulou, G. Sakellariopoulos, *Fuel*, 88(1) (2009) 195–205
- 309 [16] M. J. De Witt, L. J. Broadbelt, *Energ. Fuel*, 14 (2000) 448-458
- 310 [17] I. Johannes, H. Tamvelius, L. Tiikma, *J. Anal. Appl. Pyrolysis* 72 (2004) 113-119
- 311 [18] P. Paik, K.K. Kar, *Mater. Chem. Phys.* 113 (2009) 953-961
- 312 [19] P. Budrugaec, *Thermochim. Acta* 500 (2010) 30-37
- 313 [20] S. Kim, E.-S. Jang, D.-H. Shin, K.-H. Lee, *Polym. Degrad. Stabil.*, 85(2) (2004) 799–805
- 314 [21] J. Yang, R. Miranda, C. Roy, *Polym. Degrad. Stabil.*, 73(3) (2001) 455–461.
- 315 [22] N. Gascoin, Etude et mesure de paramètres pertinents dans un écoulement réactif application au
316 refroidissement par endo-carburant d'un super-statoréacteur, Editions Universitaires Européennes, April
317 2010, ISBN13: 978-6131501074, p.376
- 318 [23] N. Gascoin, A. Navarro-Rodriguez, G. Fau, P. Gillard, *Polym. Degrad. Stabil.*, 97 (2012) 1142-1150
- 319 [24] T. P. Wampler, *Applied Pyrolysis Handbook*, 2007 Taylor & Francis Group LLC
- 320 [25] T.P. Wampler, E.J. Levy, *J. Anal. Appl. Pyrolysis*, 8 (1985), 153-161
- 321 [26] T. Hayakawa, S. Kageyama, M.L. Puri, *J. Stat. Plan. Infer.* 138 (11) (2008) 3293.
- 322 [27] A. Mangeot, Étude expérimentale et développement numérique d'une modélisation des phénomènes
323 physicochimiques dans un propulseur hybride spatial, Ph.D. Thesis, December 2012, University of Orléans,
324 France.
- 325 [28] G. Abraham, Etude et développement d'une méthode d'analyse par spectroscopie infrarouge appliquée à la
326 pyrolyse d'hydrocarbures en conditions supercritiques et transitoires, Ph.D. Thesis, University of Orléans,
327 France, December 2009
- 328 [29] International Security data for HDPE, <http://www.cdc.gov/niosh/ipcsnfrn/nfrn1488.html>, last accessed
329 11/01/2013
- 330 [30] O. Senneca, R. Chirone, P. Salatino, *J. Anal. Appl. Pyrol.*, 71(2) (2004) 959–970
- 331 [31] G. Fau, N. Gascoin, P. Gillard, M. Bouchez, J. Steelant, *J. Anal. Appl. Pyrol.*, 95 (2012) 180–188
- 332

- 333
- 334 Table 1. List and levels of physical parameters of the design of experiments.
- 335 Table 2. TG pyrolysis data of HDPE under inert and oxidative conditions.
- 336 Table 3. Mole fractions (mol. %) of HDPE pyrolysis products under corresponding test conditions.
- 337 Table 4. Example of data post-processing according to the design of experiments for ethylene formation.
- 338 Table 5. Parameters effect on the formation of pyrolysis products (in mol. %).
- 339
- 340 Figure 1. Reproducibility tests on TG analysis under inert atmosphere at 420 °C with different sample size (a) and on
- 341 Flash Pyrolysis (b).
- 342 Figure 2. TGA mass loss divided by the sample mass under oxidative atmosphere.
- 343 Figure 3. Regression rate measured by TG (a) and converted in mm.s⁻¹ for hybrid rocket application (b).
- 344 Figure 4. Mass spectrogram of HDPE pyrolysis mixtures obtained at 20000 K/s for some test conditions.
- 345 Figure 5. Formation of alkenes, alkanes and dienes under inert and oxidative atmosphere.
- 346 Figure 6. Formation of alkenes, alkanes and dienes at two pressure levels.
- 347 Figure 7. Formation of alkenes, alkanes and dienes at two heating rates.

348

Table 1. List and levels of physical parameters of the design of experiments

Level of parameter	Heating rate (K.s ⁻¹)	Pressure (MPa)	Reactant Gas	Setup Temperature (K)
-1	100	0.1	Inert (He)	1000
-	-	-	-	1250
+1	20000	3.0	Oxidative (air)	1500

349

Table 2. TG pyrolysis data of HDPE under inert and oxidative conditions.

Setup temperature (K)	Inert (Argon)			Oxidative (Air)		
	Pyrolysis rate (wt.%)	Regression rate (mg.s ⁻¹)	Regression rate (mm.s ⁻¹)	Pyrolysis rate (wt.%)	Regression rate (mg.s ⁻¹)	Regression rate (mm.s ⁻¹)
633	8 %	1.9.10 ⁻⁴	4.7.10 ⁻⁵	13 %	5.9.10 ⁻⁴	7.6.10 ⁻⁵
653	39 %	3.0.10 ⁻⁴	6.6.10 ⁻⁵	41 %	7.9.10 ⁻⁴	1.6.10 ⁻⁴
673	88 %	4.5.10 ⁻⁴	8.1.10 ⁻⁵	91 %	2.2.10 ⁻³	3.5.10 ⁻⁴
693	91 %	3.3.10 ⁻³	1.7.10 ⁻⁴	91 %	3.2.10 ⁻³	5.5.10 ⁻⁴
713	100 %	1.4.10 ⁻³	3.0.10 ⁻⁴	97 %	1.6.10 ⁻²	1.2.10 ⁻³
733	100 %	2.9.10 ⁻³	4.6.10 ⁻⁴	100 %	4.0.10 ⁻²	2.9.10 ⁻³
773	100 %	2.2.10 ⁻²	1.4.10 ⁻³	100 %	1.5.10 ⁻¹	9.3.10 ⁻³

Table 3. Mole fractions (mol. %) of HDPE pyrolysis products under corresponding test conditions.

Species	Test number: Molecular weight (g.mol ⁻¹)	1	2	3	4	5	6	7	8	9	10	11	12
		1000K 1 bar He 2.10 ⁴ K/s	1000 K 30 barHe 2.10 ⁴ K/s	1000 K 1 bar air 2.10 ⁴ K/s	1250K 1 bar He 2.10 ⁴ K/s	1250 K 30 barHe 2.10 ⁴ K/s	1250 K 1 bar air 2.10 ⁴ K/s	1500K 1 bar He 2.10 ⁴ K/s	1500 K 30 barHe 2.10 ⁴ K/s	1500 K 1 bar air 2.10 ⁴ K/s	1000K 1 bar He 100K/s	1250 K 1 bar He 100K/s	1500 K 1 bar He 100K/s
CH4	16	0.00	0.00	0.00	0.00	0.00	0.00	0.00	0.00	0.00	0.00	0.00	0.00
C2H2	26	0.00	0.00	0.00	0.00	0.07	0.00	0.00	0.00	0.00	0.00	0.00	0.00
C2H4	28	3.20	45.95	0.97	1.40	38.38	0.85	1.33	14.78	0.76	0.49	1.58	4.28
C2H6	30	1.19	18.47	0.58	0.40	13.50	0.20	0.42	8.27	0.18	0.30	0.66	1.16
C3H6	42	9.98	12.41	10.64	8.09	7.52	11.96	10.94	11.04	10.75	5.51	7.85	17.52
C3H8	44	9.66	2.98	5.98	3.41	2.89	4.54	6.31	4.71	4.08	4.68	4.88	4.32
C4H8	56	2.01	1.78	3.73	3.61	0.60	5.82	2.25	3.09	5.23	1.81	3.04	10.58
C4H10	58	1.94	0.34	0.15	0.48	0.10	0.70	0.63	0.27	0.63	0.49	0.43	0.38
C5H10	70	0.80	0.25	0.29	0.20	0.32	0.30	0.00	0.56	0.27	0.07	0.15	0.94
C5H12	72	0.00	0.28	0.47	0.36	0.34	0.54	0.46	0.36	0.48	0.47	0.54	0.44
C6H12	84	1.46	3.92	0.79	2.98	7.66	4.77	3.18	12.89	4.29	0.65	2.36	5.63
C6H14	86	1.73	0.17	0.73	0.62	0.23	0.63	0.84	0.29	0.57	0.83	0.91	0.61
C7H14	96	1.50	0.64	0.18	0.28	0.67	0.25	0.09	1.56	0.22	0.06	0.17	0.54
C7H16	98	0.55	0.12	0.81	0.64	0.15	0.59	0.72	0.24	0.53	0.77	0.82	0.59
C8	113	0.00	0.00	8.10	5.55	0.00	5.50	4.90	4.62	2.67	0.89	6.48	1.68
C9H16	124	0.00	0.00	1.31	0.92	0.00	0.00	0.00	0.00	1.81	0.00	0.00	0.98
C9H18	126	12.20	2.86	2.64	4.49	2.45	9.31	6.48	6.51	8.47	9.52	9.75	5.03
C9H20	128	4.38	0.97	3.78	2.52	0.49	2.17	2.68	1.36	3.03	3.93	3.79	1.56
C10H18	138	2.16	0.00	3.77	2.69	2.73	3.96	3.70	3.36	3.89	2.64	2.74	3.79
C10H20	140	16.47	4.69	8.66	9.25	6.51	9.81	14.40	7.30	9.52	11.80	12.44	9.12
C10H22	142	8.05	1.52	3.96	2.57	1.81	2.82	4.63	1.58	3.45	4.01	4.11	1.64
C11H20	152	0.00	0.00	2.26	1.74	1.76	2.54	1.73	2.00	2.29	1.70	1.86	2.34
C11H22	154	7.58	1.99	5.03	5.43	3.94	5.68	7.42	4.07	5.46	6.47	6.54	4.86
C11H24	156	6.31	0.61	4.12	2.69	1.84	2.57	4.58	1.51	3.18	4.17	4.44	1.57
C12H22	166	0.00	0.00	2.13	1.48	1.25	1.96	1.40	1.79	2.08	1.25	1.40	2.21
C12H24	168	1.19	0.00	2.90	2.47	1.73	2.36	2.49	2.07	2.68	2.91	2.77	2.28
C12H26	170	1.87	0.00	3.16	2.24	1.20	2.47	2.68	1.01	1.99	3.08	2.87	1.16
C13H24	180	0.00	0.00	2.04	1.42	0.59	1.26	0.58	1.05	1.67	1.02	0.96	1.47
C13H26	182	0.00	0.00	2.53	1.83	0.73	1.43	0.89	1.16	2.00	1.81	1.64	1.46
C13H28	184	0.00	0.00	2.27	1.12	0.46	0.72	1.13	0.49	1.33	1.45	1.38	0.59
C14H26	194	0.00	0.00	1.74	0.98	0.08	1.10	0.00	0.52	1.49	0.73	0.61	0.90
C14H28	196	0.00	0.00	2.10	1.52	0.00	1.06	1.14	0.52	1.67	1.52	1.31	1.00
C15	210	1.77	0.00	2.17	2.64	0.00	2.44	3.25	1.00	2.32	3.06	1.85	1.66
C16	224	1.78	0.00	1.96	2.52	0.00	1.69	1.81	0.00	1.78	2.81	0.73	1.25
C17	238	1.79	0.00	2.24	2.44	0.00	1.94	2.13	0.00	1.80	2.44	1.47	1.12
C18	252	0.43	0.00	1.77	2.60	0.00	1.26	1.01	0.00	1.72	2.43	0.65	0.93
C19	267	0.00	0.00	1.31	2.60	0.00	1.05	1.67	0.00	1.03	2.24	0.58	0.70
C20	281	0.00	0.00	1.39	2.80	0.00	0.58	0.74	0.00	0.89	3.07	0.44	0.60
C21	295	0.00	0.00	1.05	4.26	0.00	0.60	0.47	0.00	1.52	3.46	1.49	0.55
C22	309	0.00	0.00	0.20	2.76	0.00	1.59	0.76	0.00	0.95	2.82	1.96	0.89
C23	323	0.00	0.00	0.00	2.30	0.00	0.76	0.00	0.00	0.77	2.12	1.44	0.59
C24	337	0.00	0.00	0.00	1.48	0.00	0.14	0.00	0.00	0.47	0.16	0.82	0.75
C25	351	0.00	0.00	0.00	0.08	0.00	0.00	0.00	0.00	0.00	0.30	0.00	0.27
C26	365	0.00	0.00	0.00	0.00	0.00	0.00	0.00	0.00	0.00	0.00	0.00	0.00
Alkanes		35.68	25.47	26.01	17.04	22.98	17.95	25.07	20.09	19.45	24.17	24.83	14.03
Alkenes		62.17	74.48	60.65	73.60	70.52	71.13	67.36	71.17	67.24	68.44	67.52	74.23
Dienes		2.16	0.00	13.26	9.23	6.48	10.82	7.41	8.72	13.23	7.35	7.58	11.69

353

354

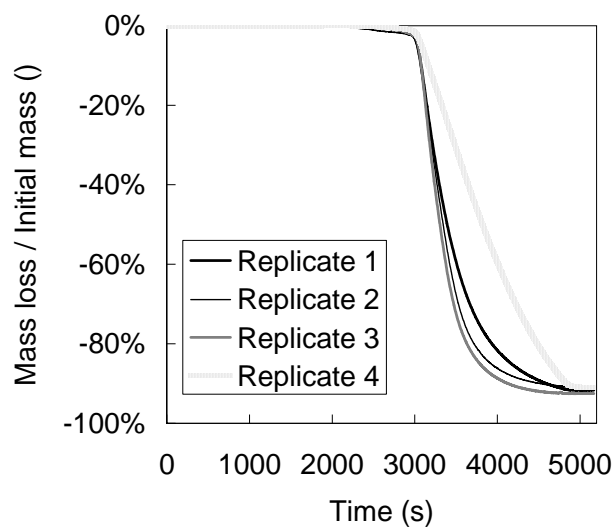
Table 4. Example of data post-processing according to the design of experiments for ethylene formation.

Test number (see Table 3)	Pressure	Temperature	Heating rate	Atmosphere	C2H4 mole fraction
1	-1	-1	+1	-1	3.2%
2	+1	-1	+1	-1	45.9%
3	-1	-1	+1	+1	1.0%
7	-1	+1	+1	-1	1.3%
8	+1	+1	+1	-1	14.8%
9	-1	+1	+1	+1	0.8%
10	-1	-1	-1	-1	0.5%
12	-1	+1	-1	-1	4.3%
Parameters effects :	49.7%	-29.5%	62.2%	-68.3%	9.0 %

355

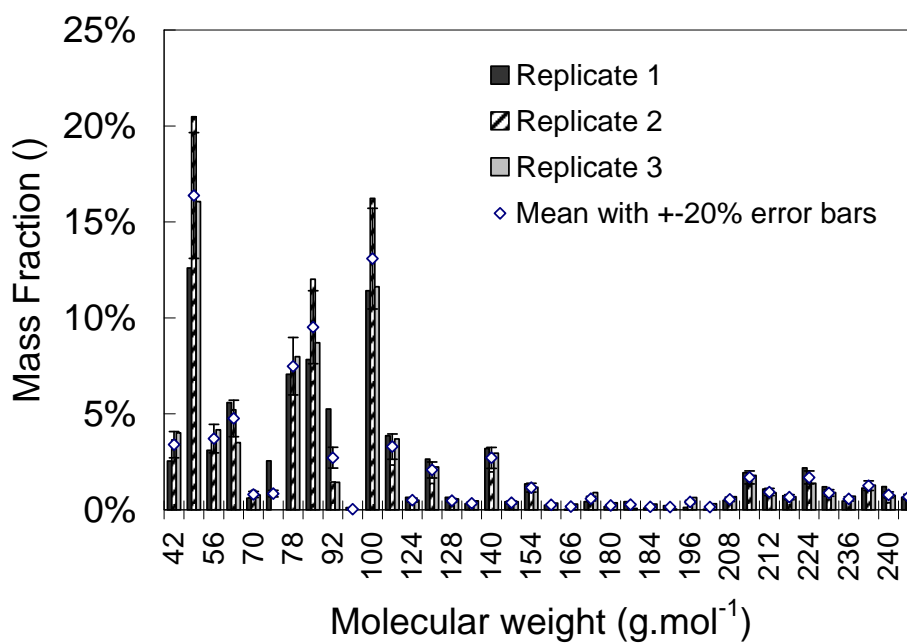
Table 5. Parameters effect on the formation of pyrolysis products (in mol. %).

	Pressure	Temperature	Heating rate	Atmosphere	Mean mole fraction
C2H4	49.7%	-29.5%	62.2%	-68.3%	9.0%
C2H6	22.9%	-10.5%	27.6%	-29.0%	3.8%
C3H6	-41.9%	11.7%	42.7%	-46.0%	11.1%
C3H8	-27.3%	-3.9%	24.7%	-22.6%	5.3%
C4H8	-20.75%	11.81%	5.70%	-12.55%	3.81%
C4H10	-3.6%	-1.0%	3.1%	-3.3%	0.6%
C5H10	-1.5%	0.4%	1.2%	-2.1%	0.4%
C5H12	-1.7%	0.5%	1.2%	-1.1%	0.4%
C6H12	0.8%	19.2%	20.3%	-22.7%	4.1%
C6H14	-4.8%	-1.1%	2.9%	-3.2%	0.7%
C7H14	-0.4%	0.0%	3.6%	-4.0%	0.6%
C7H16	-3.6%	-0.2%	1.6%	-1.6%	0.5%
C8	-13.6%	4.9%	17.7%	-1.3%	2.9%
C9H16	-4.1%	1.5%	2.1%	2.1%	0.5%
C9H18	-35.0%	-0.7%	24.6%	-31.5%	6.7%
C9H20	-17.0%	-4.4%	10.7%	-8.1%	2.7%
C10H18	-16.6%	6.2%	10.4%	-8.0%	2.9%
C10H20	-58.0%	-1.3%	40.1%	-45.6%	10.2%
C10H22	-22.6%	-6.2%	17.5%	-14.0%	3.6%
C11H20	-8.3%	4.4%	4.2%	-3.2%	1.5%
C11H22	-30.8%	0.7%	20.2%	-21.9%	5.4%
C11H24	-21.8%	-4.4%	14.6%	-11.4%	3.3%
C12H22	-7.3%	4.1%	3.9%	-2.4%	1.4%
C12H24	-12.4%	2.5%	6.1%	-5.4%	2.1%
C12H26	-12.9%	-1.3%	6.5%	-4.7%	1.9%
C13H24	-5.7%	1.7%	2.9%	-0.4%	1.0%
C13H26	-7.5%	1.2%	3.3%	-0.8%	1.2%
C13H28	-6.3%	-0.2%	3.2%	-0.1%	0.9%
C14H26	-4.3%	0.4%	2.1%	1.1%	0.7%
C14H28	-6.9%	0.7%	2.9%	-0.4%	1.0%
C15	-13.2%	1.2%	5.8%	-6.3%	1.9%
C16	-11.4%	-1.7%	3.3%	-3.9%	1.4%
C17	-11.5%	-1.4%	4.4%	-3.5%	1.4%
C18	-8.3%	-1.0%	1.6%	-1.3%	1.0%
C19	-7.0%	-0.1%	1.1%	-2.3%	0.9%
C20	-6.7%	-2.2%	-0.7%	-2.1%	0.8%
C21	-7.1%	-2.0%	-1.0%	-1.9%	0.9%
C22	-5.6%	-0.4%	-1.8%	-3.3%	0.7%
C23	-3.5%	-0.8%	-1.9%	-1.9%	0.4%
C24	-1.4%	1.1%	-0.4%	-0.4%	0.2%
C25	-0.6%	0.0%	-0.6%	-0.6%	0.1%
C26	0.0%	0.0%	0.0%	0.0%	0.0%



358

a)

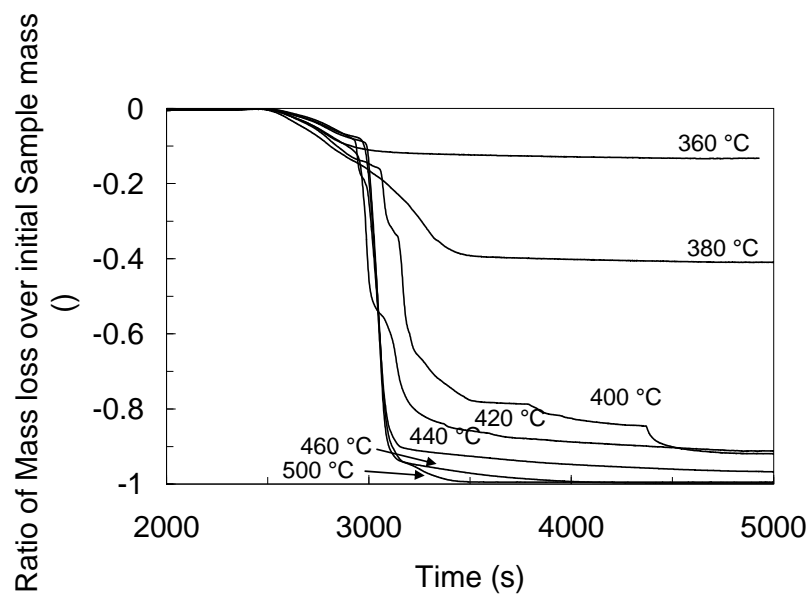


359

b)

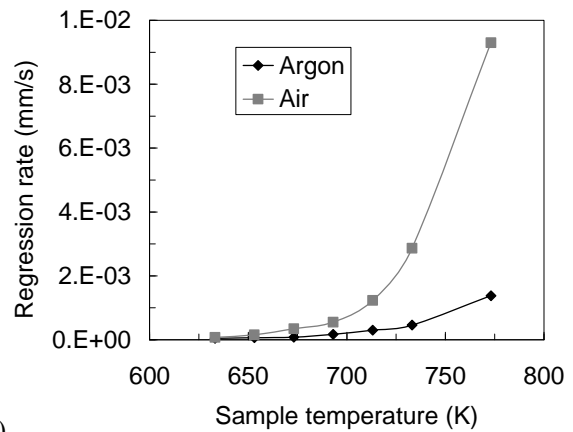
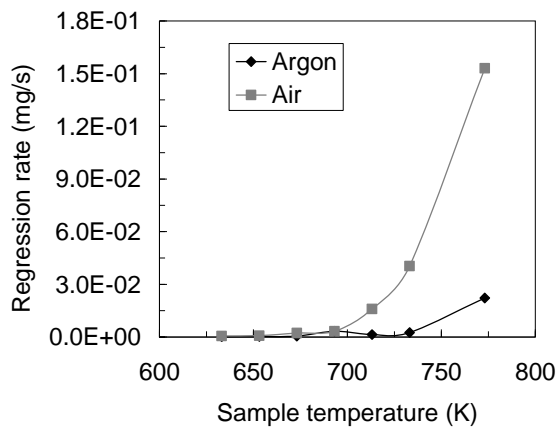
360 **Figure 1. Reproducibility tests on TG analysis under inert atmosphere at 420 °C with different sample size (a)**

361 **and on Flash Pyrolysis (b).**



362
363

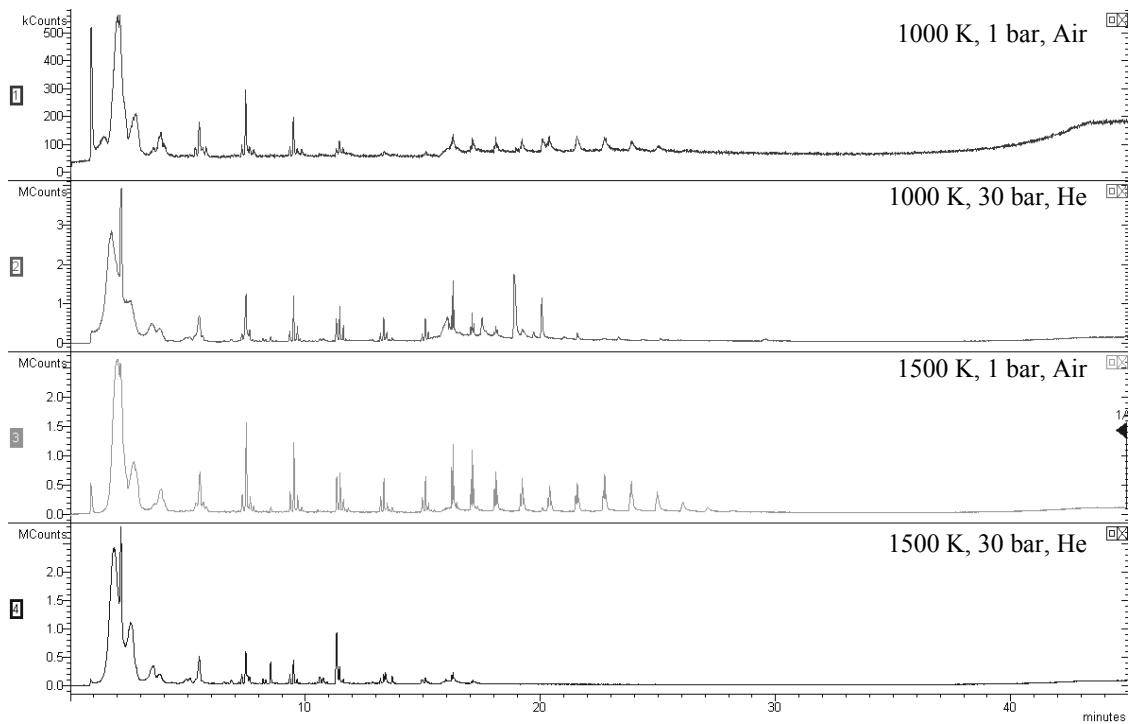
Figure 2. TGA mass loss divided by the sample mass under oxidative atmosphere.



364

365

Figure 3. Regression rate measured by TG (a) and converted in $\text{mm}\cdot\text{s}^{-1}$ for hybrid rocket application (b).

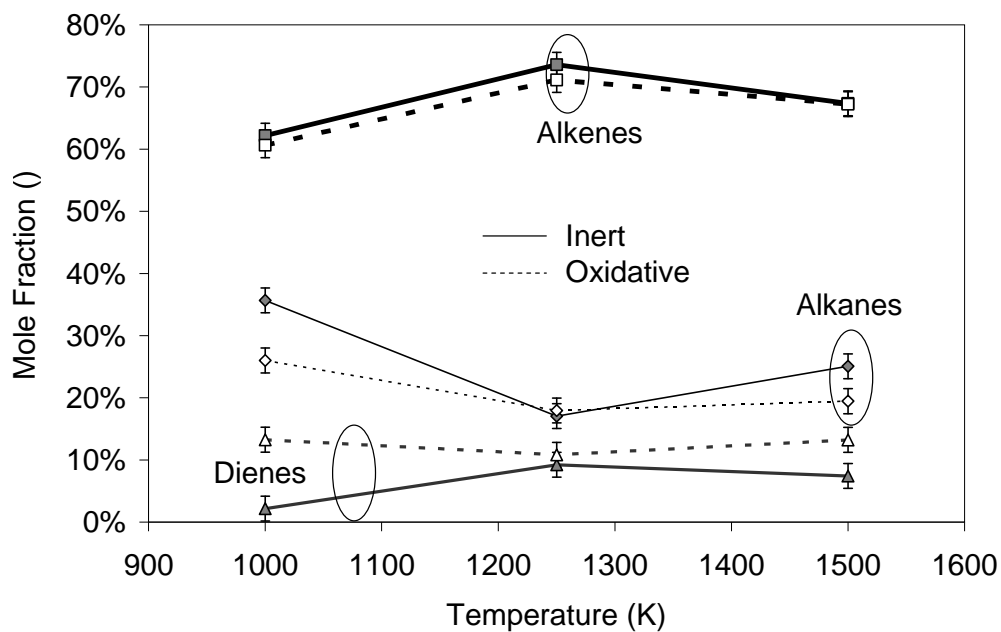


366

367

368

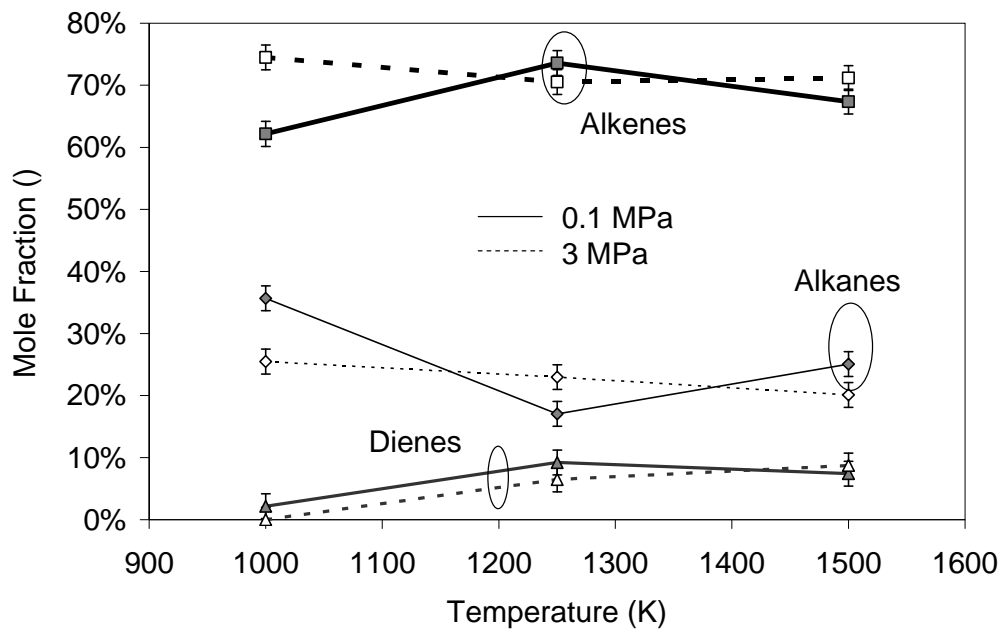
Figure 4. Mass spectrogram of HDPE pyrolysis mixtures obtained at 20000 K/s for some test conditions.



369

370

Figure 5. Formation of alkenes, alkanes and dienes under inert and oxidative atmosphere.



371
372

Figure 6. Formation of alkenes, alkanes and dienes at two pressure levels.

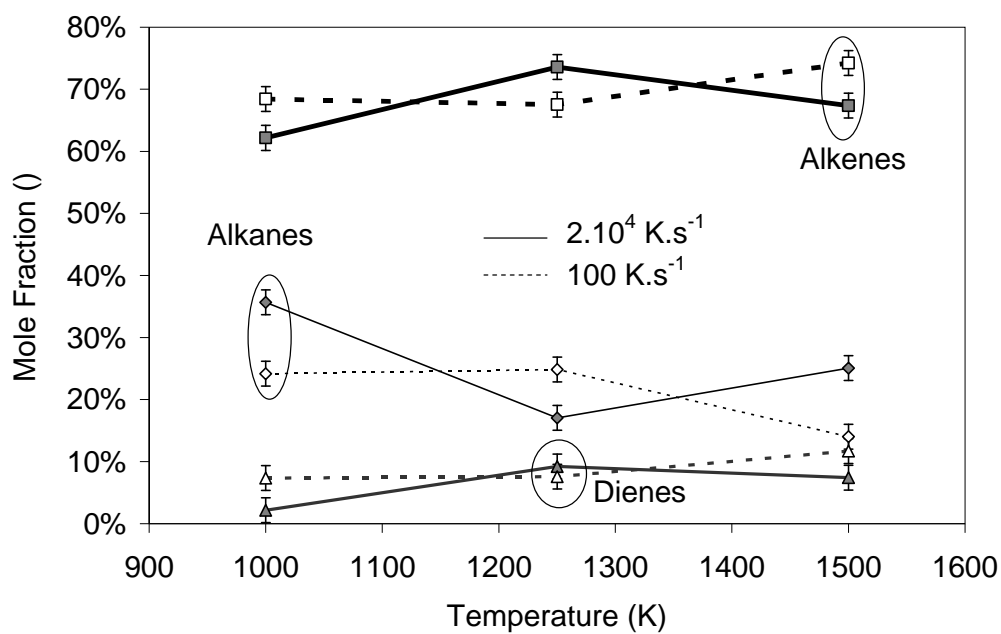


Figure 7. Formation of alkenes, alkanes and dienes at two heating rates.

373

374

375